

Search for $B^0 \rightarrow K^{*0} \nu \bar{\nu}$ Using One Fully Reconstructed B Meson

K. Abe,⁹ K. Abe,⁴⁹ I. Adachi,⁹ H. Aihara,⁵¹ D. Anipko,¹ K. Aoki,²⁵ T. Arakawa,³²
 K. Arinstein,¹ Y. Asano,⁵⁶ T. Aso,⁵⁵ V. Aulchenko,¹ T. Aushev,²¹ T. Aziz,⁴⁷ S. Bahinipati,⁴
 A. M. Bakich,⁴⁶ V. Balagura,¹⁵ Y. Ban,³⁷ S. Banerjee,⁴⁷ E. Barberio,²⁴ M. Barbero,⁸
 A. Bay,²¹ I. Bedny,¹ K. Belous,¹⁴ U. Bitenc,¹⁶ I. Bizjak,¹⁶ S. Blyth,²⁷ A. Bondar,¹
 A. Bozek,³⁰ M. Bračko,^{23,16} J. Brodzicka,^{9,30} T. E. Browder,⁸ M.-C. Chang,⁵⁰ P. Chang,²⁹
 Y. Chao,²⁹ A. Chen,²⁷ K.-F. Chen,²⁹ W. T. Chen,²⁷ B. G. Cheon,³ R. Chistov,¹⁵
 J. H. Choi,¹⁸ S.-K. Choi,⁷ Y. Choi,⁴⁵ Y. K. Choi,⁴⁵ A. Chuvikov,³⁹ S. Cole,⁴⁶ J. Dalseno,²⁴
 M. Danilov,¹⁵ M. Dash,⁵⁷ R. Dowd,²⁴ J. Dragic,⁹ A. Druts koy,⁴ S. Eidelman,¹ Y. Enari,²⁵
 D. Epifanov,¹ S. Fratina,¹⁶ H. Fujii,⁹ M. Fujikawa,²⁶ N. Gabyshev,¹ A. Garmash,³⁹
 T. Gershon,⁹ A. Go,²⁷ G. Gokhroo,⁴⁷ P. Goldenzweig,⁴ B. Golob,^{22,16} A. Gorišek,¹⁶
 M. Grosse Perdekamp,^{11,40} H. Guler,⁸ H. Ha,¹⁸ J. Haba,⁹ K. Hara,²⁵ T. Hara,³⁵
 Y. Hasegawa,⁴⁴ N. C. Hastings,⁵¹ K. Hayasaka,²⁵ H. Hayashii,²⁶ M. Hazumi,⁹
 D. Heffernan,³⁵ T. Higuchi,⁹ L. Hinz,²¹ T. Hokuue,²⁵ Y. Hoshi,⁴⁹ K. Hoshina,⁵⁴ S. Hou,²⁷
 W.-S. Hou,²⁹ Y. B. Hsiung,²⁹ Y. Igarashi,⁹ T. Iijima,²⁵ K. Ikado,²⁵ A. Imoto,²⁶ K. Inami,²⁵
 A. Ishikawa,⁵¹ H. Ishino,⁵² K. Itoh,⁵¹ R. Itoh,⁹ M. Iwabuchi,⁶ M. Iwasaki,⁵¹ Y. Iwasaki,⁹
 C. Jacoby,²¹ M. Jones,⁸ H. Kakuno,⁵¹ J. H. Kang,⁵⁸ J. S. Kang,¹⁸ P. Kapusta,³⁰
 S. U. Kataoka,²⁶ N. Katayama,⁹ H. Kawai,² T. Kawasaki,³² H. R. Khan,⁵² A. Kibayashi,⁵²
 H. Kichimi,⁹ N. Kikuchi,⁵⁰ H. J. Kim,²⁰ H. O. Kim,⁴⁵ J. H. Kim,⁴⁵ S. K. Kim,⁴³
 T. H. Kim,⁵⁸ Y. J. Kim,⁶ K. Kinoshita,⁴ N. Kishimoto,²⁵ S. Korpar,^{23,16} Y. Kozakai,²⁵
 P. Križan,^{22,16} P. Krokovny,⁹ T. Kubota,²⁵ R. Kulasiri,⁴ R. Kumar,³⁶ C. C. Kuo,²⁷
 E. Kurihara,² A. Kusaka,⁵¹ A. Kuzmin,¹ Y.-J. Kwon,⁵⁸ J. S. Lange,⁵ G. Leder,¹³ J. Lee,⁴³
 S. E. Lee,⁴³ Y.-J. Lee,²⁹ T. Lesiak,³⁰ J. Li,⁸ A. Limosani,⁹ C. Y. Lin,²⁹ S.-W. Lin,²⁹
 Y. Liu,⁶ D. Liventsev,¹⁵ J. MacNaughton,¹³ G. Majumder,⁴⁷ F. Mandl,¹³ D. Marlow,³⁹
 T. Matsumoto,⁵³ A. Matyja,³⁰ S. McOnie,⁴⁶ T. Medvedeva,¹⁵ Y. Mikami,⁵⁰ W. Mitaroff,¹³
 K. Miyabayashi,²⁶ H. Miyake,³⁵ H. Miyata,³² Y. Miyazaki,²⁵ R. Mizuk,¹⁵ D. Mohapatra,⁵⁷
 G. R. Moloney,²⁴ T. Mori,⁵² J. Mueller,³⁸ A. Murakami,⁴¹ T. Nagamine,⁵⁰ Y. Nagasaka,¹⁰
 T. Nakagawa,⁵³ Y. Nakahama,⁵¹ I. Nakamura,⁹ E. Nakano,³⁴ M. Nakao,⁹ H. Nakazawa,⁹
 Z. Natkaniec,³⁰ K. Neichi,⁴⁹ S. Nishida,⁹ K. Nishimura,⁸ O. Nitoh,⁵⁴ S. Noguchi,²⁶
 T. Nozaki,⁹ A. Ogawa,⁴⁰ S. Ogawa,⁴⁸ T. Ohshima,²⁵ T. Okabe,²⁵ S. Okuno,¹⁷ S. L. Olsen,⁸
 S. Ono,⁵² W. Ostrowicz,³⁰ H. Ozaki,⁹ P. Pakhlov,¹⁵ G. Pakhlova,¹⁵ H. Palka,³⁰
 C. W. Park,⁴⁵ H. Park,²⁰ K. S. Park,⁴⁵ N. Parslow,⁴⁶ L. S. Peak,⁴⁶ M. Pernicka,¹³
 R. Pestotnik,¹⁶ M. Peters,⁸ L. E. Piilonen,⁵⁷ A. Poluektov,¹ F. J. Ronga,⁹ N. Root,¹
 J. Rorie,⁸ M. Rozanska,³⁰ H. Sahoo,⁸ S. Saitoh,⁹ Y. Sakai,⁹ H. Sakamoto,¹⁹ H. Sakaue,³⁴
 T. R. Sarangi,⁶ N. Sato,²⁵ N. Satoyama,⁴⁴ K. Sayeed,⁴ T. Schietinger,²¹ O. Schneider,²¹
 P. Schönmeier,⁵⁰ J. Schümann,²⁸ C. Schwanda,¹³ A. J. Schwartz,⁴ R. Seidl,^{11,40} T. Seki,⁵³
 K. Senyo,²⁵ M. E. Sevier,²⁴ M. Shapkin,¹⁴ Y.-T. Shen,²⁹ H. Shibuya,⁴⁸ B. Shwartz,¹
 V. Sidorov,¹ J. B. Singh,³⁶ A. Sokolov,¹⁴ A. Somov,⁴ N. Soni,³⁶ R. Stamen,⁹ S. Stanič,³³
 M. Starič,¹⁶ H. Stoeck,⁴⁶ A. Sugiyama,⁴¹ K. Sumisawa,⁹ T. Sumiyoshi,⁵³ S. Suzuki,⁴¹
 S. Y. Suzuki,⁹ O. Tajima,⁹ N. Takada,⁴⁴ F. Takasaki,⁹ K. Tamai,⁹ N. Tamura,³²
 K. Tanabe,⁵¹ M. Tanaka,⁹ G. N. Taylor,²⁴ Y. Teramoto,³⁴ X. C. Tian,³⁷ I. Tikhomirov,¹⁵

K. Trabelsi,⁹ Y. T. Tsai,²⁹ Y. F. Tse,²⁴ T. Tsuboyama,⁹ T. Tsukamoto,⁹ K. Uchida,⁸
 Y. Uchida,⁶ S. Uehara,⁹ T. Uglov,¹⁵ K. Ueno,²⁹ Y. Unno,⁹ S. Uno,⁹ P. Urquijo,²⁴
 Y. Ushiroda,⁹ Y. Usov,¹ G. Varner,⁸ K. E. Varvell,⁴⁶ S. Villa,²¹ C. C. Wang,²⁹
 C. H. Wang,²⁸ M.-Z. Wang,²⁹ M. Watanabe,³² Y. Watanabe,⁵² J. Wicht,²¹ L. Widhalm,¹³
 J. Wiechczynski,³⁰ E. Won,¹⁸ C.-H. Wu,²⁹ Q. L. Xie,¹² B. D. Yabsley,⁴⁶ A. Yamaguchi,⁵⁰
 H. Yamamoto,⁵⁰ S. Yamamoto,⁵³ Y. Yamashita,³¹ M. Yamauchi,⁹ Heyoung Yang,⁴³
 S. Yoshino,²⁵ Y. Yuan,¹² Y. Yusa,⁵⁷ S. L. Zang,¹² C. C. Zhang,¹² J. Zhang,⁹
 L. M. Zhang,⁴² Z. P. Zhang,⁴² V. Zhilich,¹ T. Ziegler,³⁹ A. Zupanc,¹⁶ and D. Zürcher²¹

(The Belle Collaboration)

(Belle Collaboration)

¹*Budker Institute of Nuclear Physics, Novosibirsk*

²*Chiba University, Chiba*

³*Chonnam National University, Kwangju*

⁴*University of Cincinnati, Cincinnati, Ohio 45221*

⁵*University of Frankfurt, Frankfurt*

⁶*The Graduate University for Advanced Studies, Hayama*

⁷*Gyeongsang National University, Chinju*

⁸*University of Hawaii, Honolulu, Hawaii 96822*

⁹*High Energy Accelerator Research Organization (KEK), Tsukuba*

¹⁰*Hiroshima Institute of Technology, Hiroshima*

¹¹*University of Illinois at Urbana-Champaign, Urbana, Illinois 61801*

¹²*Institute of High Energy Physics,*

Chinese Academy of Sciences, Beijing

¹³*Institute of High Energy Physics, Vienna*

¹⁴*Institute of High Energy Physics, Protvino*

¹⁵*Institute for Theoretical and Experimental Physics, Moscow*

¹⁶*J. Stefan Institute, Ljubljana*

¹⁷*Kanagawa University, Yokohama*

¹⁸*Korea University, Seoul*

¹⁹*Kyoto University, Kyoto*

²⁰*Kyungpook National University, Taegu*

²¹*Swiss Federal Institute of Technology of Lausanne, EPFL, Lausanne*

²²*University of Ljubljana, Ljubljana*

²³*University of Maribor, Maribor*

²⁴*University of Melbourne, Victoria*

²⁵*Nagoya University, Nagoya*

²⁶*Nara Women's University, Nara*

²⁷*National Central University, Chung-li*

²⁸*National United University, Miao Li*

²⁹*Department of Physics, National Taiwan University, Taipei*

³⁰*H. Niewodniczanski Institute of Nuclear Physics, Krakow*

³¹*Nippon Dental University, Niigata*

³²*Niigata University, Niigata*

³³*University of Nova Gorica, Nova Gorica*

³⁴*Osaka City University, Osaka*

- ³⁵*Osaka University, Osaka*
³⁶*Panjab University, Chandigarh*
³⁷*Peking University, Beijing*
³⁸*University of Pittsburgh, Pittsburgh, Pennsylvania 15260*
³⁹*Princeton University, Princeton, New Jersey 08544*
⁴⁰*RIKEN BNL Research Center, Upton, New York 11973*
⁴¹*Saga University, Saga*
⁴²*University of Science and Technology of China, Hefei*
⁴³*Seoul National University, Seoul*
⁴⁴*Shinshu University, Nagano*
⁴⁵*Sungkyunkwan University, Suwon*
⁴⁶*University of Sydney, Sydney NSW*
⁴⁷*Tata Institute of Fundamental Research, Bombay*
⁴⁸*Toho University, Funabashi*
⁴⁹*Tohoku Gakuin University, Tagajo*
⁵⁰*Tohoku University, Sendai*
⁵¹*Department of Physics, University of Tokyo, Tokyo*
⁵²*Tokyo Institute of Technology, Tokyo*
⁵³*Tokyo Metropolitan University, Tokyo*
⁵⁴*Tokyo University of Agriculture and Technology, Tokyo*
⁵⁵*Toyama National College of Maritime Technology, Toyama*
⁵⁶*University of Tsukuba, Tsukuba*
⁵⁷*Virginia Polytechnic Institute and State University, Blacksburg, Virginia 24061*
⁵⁸*Yonsei University, Seoul*

Abstract

We present a search for the rare decay $B^0 \rightarrow K^{*0} \nu \bar{\nu}$, using a data sample of 492 fb^{-1} collected with the Belle detector at the KEKB e^+e^- collider. Signal candidates are required to have an accompanying B meson fully reconstructed in one of the hadronic modes and signal-side particles consistent with a single K^{*0} meson. No significant signal is observed in the data sample and we set a 90% confidence level upper limit of 3.4×10^{-4} on the branching fraction.

PACS numbers: 13.25.Hw, 14.40.Nd

The decays $B \rightarrow K^{(*)}\nu\bar{\nu}$ and $B \rightarrow K^{(*)}l^+l^-$ proceed through the flavor-changing neutral-current processes, which are sensitive to physics beyond the Standard Model (SM) associated penguin loops. In the SM, the dominant diagram of these decays is the penguin process shown in Figure 1 a). The SM branching fractions are estimated to be around the $10^{-5}/10^{-6}$ level for the K^*/K modes based on next-to-leading-order calculations [1]. Calculation of the decay amplitudes for $B \rightarrow K^{(*)}\nu\bar{\nu}$ is particularly clean theoretically, owing to the absence of long-distance interactions that affect the charged-lepton channels $B \rightarrow K^{(*)}l^+l^-$. New physics such as SUSY particles or the effect of a possible fourth generation could potentially contribute to the penguin loop or box diagram (Figure 1 b)) to enhance the branching fractions [1]. Reference [2] also discusses the possibility of discovering light dark matter in $b \rightarrow s$ transitions with large missing momentum.

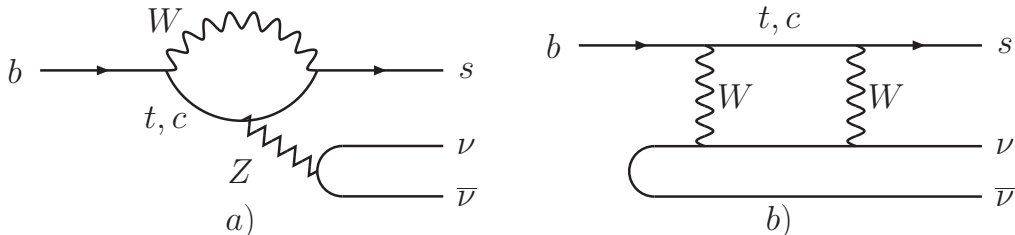


FIG. 1: The quark-level diagrams for $B \rightarrow K^*\nu\bar{\nu}$ decays.

Experimental measurements [3] of the $b \rightarrow s$ transitions with two charged leptons are in good agreement with SM calculations [1]. Further investigation of the forward-backward asymmetry in $B \rightarrow K^*l^+l^-$ [4] prefers the SM prediction although the statistics are still limited. Due to the challenge of cleanly detecting rare modes with two final-state neutrinos, only a few studies of $K^{(*)}\nu\bar{\nu}$ have been carried out to date [5]. In this paper, we report our first search for the decay $B^0 \rightarrow K^{*0}\nu\bar{\nu}$ using a data sample of 492 fb^{-1} integrated luminosity recorded at the $\Upsilon(4S)$ resonance, corresponding to 535×10^6 B -meson pairs.

The Belle detector is a large-solid-angle magnetic spectrometer located at the KEKB collider [6], and consists of a silicon vertex detector (SVD), a 50-layer central drift chamber (CDC), an array of aerogel threshold Cherenkov counters (ACC), a barrel-like arrangement of time-of-flight scintillation counters (TOF), and an electromagnetic calorimeter comprised of CsI(Tl) crystals (ECL) located inside a superconducting solenoid that provides a 1.5 T magnetic field. An iron flux-return located outside of the coil is instrumented to detect K_L^0 mesons and to identify muons (KLM). The detector is described in detail elsewhere [7].

One of the B mesons in the event is fully reconstructed as the tag-side B candidate (B_{tag}). The rest of the particles are assumed to be products of the signal-side B meson (B_{sig}). The B_{tag} candidates are reconstructed in one of the following decays: $B^0 \rightarrow D^{(*)-}\pi^+$, $D^{(*)-}\rho^+$, $D^{(*)-}a_1^+$, and $D^{(*)-}D_s^{(*)+}$. The D^- mesons are reconstructed as $D^- \rightarrow K_S^0\pi^-$, $K_S^0\pi^-\pi^0$, $K_S^0\pi^-\pi^+\pi^-$, $K^+\pi^-\pi^-$, and $K^+\pi^-\pi^-\pi^0$. The D^{*-} mesons are reconstructed as $\bar{D}^0\pi^-$, and the following decay channels are included for the \bar{D}^0 mesons: $\bar{D}^0 \rightarrow K^+\pi^-$, $K^+\pi^-\pi^0$, $K^+\pi^-\pi^+\pi^-$, $K_S^0\pi^0$, $K_S^0\pi^-\pi^+$, $K_S^0\pi^-\pi^+\pi^0$ and K^-K^+ . Furthermore, the $D_s^+ \rightarrow K_S^0K^+$ and $K^+K^-\pi^+$ decays are used for D_s^+ mesons and $D_s^{*+} \rightarrow D_s^+\gamma$ decay are also selected. A candidate B_{tag} meson is selected with the beam constrained mass $M_{\text{bc}} \equiv \sqrt{E_{\text{beam}}^2 - p_B^2}$ and the energy difference $\Delta E \equiv E_B - E_{\text{beam}}$, where E_B and p_B are the reconstructed energy and momentum of the B_{tag} candidate in the $\Upsilon(4S)$ center-of-mass (CM) frame, and E_{beam}

is the beam energy in the same system. The requirements on candidate B_{tag} mesons are $M_{\text{bc}} > 5.27 \text{ GeV}/c^2$ and $-80 \text{ MeV} < \Delta E < 60 \text{ MeV}$. If there are multiple B_{tag} candidates in one event, the candidate with the smallest χ^2 based on the deviations from the nominal values of ΔE , the D meson mass, and the mass difference between the D^* and the D (for the candidate with a D^* in the reconstruction) is chosen.

Once a B_{tag} candidate is reconstructed, the remaining particles are used to reconstruct a $B^0 \rightarrow K^{*0} \nu \bar{\nu}$ event. The K^{*0} candidate is reconstructed by two charged tracks with opposite charge, and one of the tracks should have a kaon likelihood greater than 0.6. The kaon likelihood is defined by $\mathcal{R}_K \equiv \mathcal{L}_K / (\mathcal{L}_K + \mathcal{L}_\pi)$, where \mathcal{L}_K (\mathcal{L}_π) denotes a combined likelihood measurement from the ACC, the TOF, and a dE/dx from the CDC for the K^\pm (π^\pm) tracks. The daughter K^\pm and π^\mp are required to have a maximum distance to the interaction point (IP) of 2 cm in the beam direction (z) and of 5 cm in the transverse plane ($r-\phi$). The invariant mass of the K^{*0} candidate should be within a $\pm 75 \text{ MeV}/c^2$ window of the nominal K^{*0} mass. No other charged tracks or π^0 candidates are allowed in the event, while a pair of photons with an invariant mass within $\pm 18.5 \text{ MeV}/c^2$ of the nominal π^0 mass where each photon has an energy greater than 50 MeV is considered a π^0 candidate. A B_{sig} candidate is selected according to the variable $E_{\text{ECL}} \equiv E_{\text{tot}} - E_{\text{rec}}$, where E_{tot} and E_{rec} are the total visible energy measured by the ECL detector and the measured energy of reconstructed objects including the B_{tag} and the signal side K^{*0} candidate, respectively. A minimum threshold of 50 (100,150) MeV on the cluster energy is applied for the barrel (forward endcap, backward endcap) region of the ECL detector. The signal region is defined by $E_{\text{ECL}} < 0.3 \text{ GeV}$ and the sideband region is given by $0.45 \text{ GeV} < E_{\text{ECL}} < 1.2 \text{ GeV}$.

The dominant background source is generic $B^0 \bar{B}^0$ decays. As shown in Figure 2, a Fisher discriminant containing three input variables ($P_{K^*}^*$, P_{miss}^* , and M_{miss}^2) is introduced to suppress the background, where $P_{K^*}^*$, P_{miss}^* , and M_{miss}^2 are the momentum of the K^* candidate in the CM frame, the missing momentum in the CM frame, and the squared missing mass. The missing momentum and missing mass are calculated using the momenta of the reconstructed B_{tag} and K^{*0} candidate. Based on a figure of merit study, the events with a Fisher discriminant value greater than -4.9 are rejected from the analysis. Furthermore, the cosine of the angle between the missing momentum in the laboratory frame and the beam pipe direction is required to be within the range -0.86 and 0.95 . These criteria suppress events with particles produced along the beam pipe. The contributions from continuum background $e^+e^- \rightarrow q\bar{q}$ ($q = u, d, c, s$) and other rare B decays such as $B^0 \rightarrow K^{*0}\gamma$ are expected to be small. Based on Monte Carlo (MC) simulations, the selection efficiency on the signal side is estimated to be 11%, while the B tagging efficiency is 0.087%. The reconstruction efficiency in this analysis is equal to the product of the selection efficiency and the B tagging efficiency.

The contribution from each background source is examined with large MC samples. The expected yields of background events in the signal region and sideband region are 4.8 ± 1.5 and 19 ± 3 events, respectively. Further details are listed in Table I. From the full experimental sample 13 events fall in the signal region and 19 events fall in the sideband region.

The signal yield is extracted by a fit to the E_{ECL} distribution. The signal probability density function (PDF) is modeled by a smooth histogram obtained from a signal MC sample, and a second order polynomial is used to describe the background distribution. An extended likelihood function is introduced

$$\mathcal{L} = \frac{e^{-(N_S+N_B)}}{N!} \prod_{i=1}^N [N_S P_S(E_{\text{ECL}}^i) + N_B P_B(E_{\text{ECL}}^i)], \quad (1)$$

where P_S and P_B denote the signal and background PDF. The signal yield, background yield, and total number of events in the fit are given by N_S , N_B , and N , respectively. We obtain a signal yield of $4.7^{+3.1}_{-2.6}$ events by maximizing the combined likelihood \mathcal{L} . The statistical significance is estimated to be 1.7σ by a comparison of the likelihood values for the best fit and a fit with zero signal yield. The E_{ECL} distribution with the fit results superimposed is shown in Figure 3. The $M(K\pi)$ distributions for the events in the signal region are also shown in Figure 4, while the momentum distributions of the reconstructed $K^{*0} \rightarrow K\pi$ candidates are given in Figure 5.

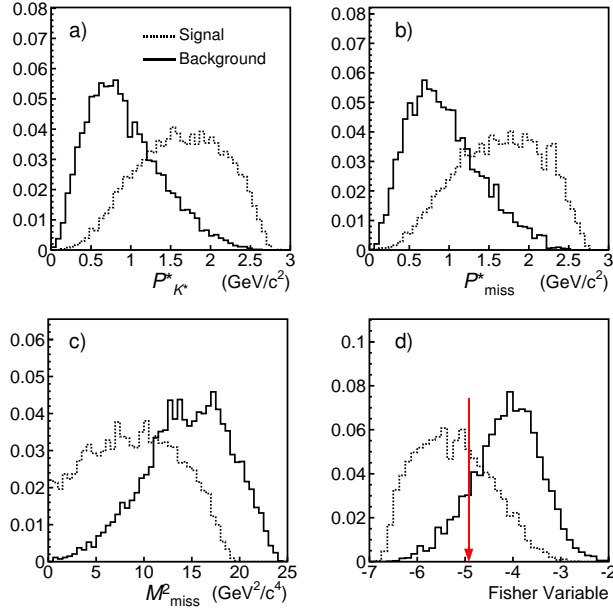


FIG. 2: The distributions for a) the momentum of K^* candidate in the CM frame ($P_{K^*}^*$), b) the missing momentum in the CM frame (P_{miss}^*), c) the squared missing mass (M_{miss}^2), and d) the Fisher discriminant (arrow indicates the cut point). The dashed (solid) lines illustrate the distributions from signal (background) MC samples.

TABLE I: The number of expected events in the signal and sideband regions.

	Signal region	Sideband region
Continuum $e^+e^- \rightarrow q\bar{q}(q = u, d, c, s)$	0.5 ± 0.5	4.8 ± 1.6
Generic $b \rightarrow c$	3.7 ± 1.4	13 ± 3
Rare B decays	0.5 ± 0.2	1.1 ± 0.3
Sum	4.8 ± 1.5	19 ± 3
Expected signal yield	0.63 ± 0.03	0.10 ± 0.01
Data	13	19

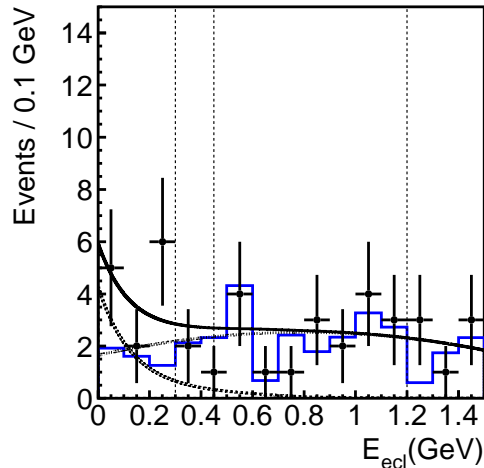


FIG. 3: The E_{ECL} distribution with fit results superimposed. The solid histogram illustrates the background distributions from MC simulations. The dashed, dotted and solid curves are the signal and background components and their sum, respectively.

The systematic uncertainty assigned for MC statistics is 3.8%. By varying the PDF parameters and repeating the fit and observing the variation of the results, we infer an error associated with the fitting procedure of 5%. The charged kaon (pion) identification is checked by a high statistics D^* tagged sample, and an error of 0.8% (1.2%) is assigned. Other possible systematic uncertainties such as tracking (2.1%) and number of $B\bar{B}$ (1%) are also included. The systematic uncertainty related to the K^* mass selection is estimated to be 4%. The total systematic uncertainty is calculated to be 7.9%. Considering the effects of both statistical and systematic errors using an extension of the Feldman Cousins method [8], we obtain an upper limit of $\mathcal{B}(B^0 \rightarrow K^{*0}\nu\bar{\nu}) < 3.4 \times 10^{-4}$ at the 90% confidence level.

In conclusion, we have performed a search for the $B^0 \rightarrow K^{*0}\nu\bar{\nu}$ decays with a fully reconstructed B tagging method on a data sample of 535×10^6 $B\bar{B}$ pairs collected at the $\Upsilon(4S)$ resonance with the Belle detector. We find $4.7_{-2.6}^{+3.1}$ signal events with a statistical significance of 1.7 standard deviations. The obtained upper limit is three times more stringent than the only published constraint [5]. Although the observed signal is much larger than the SM expectation, which is estimated to be 0.63 events in the signal region, the error is large, preventing us from drawing any conclusions at this point. We have examined several signal-like candidates and find that one of the events is consistent in missing mass with a $B^0 \rightarrow K^{*0}\gamma$ decay. The hard photon in that event hits the gap between the barrel and the forward endcap calorimeter. Further understanding of the events in the signal region will require much larger $b \rightarrow c$ MC samples in addition to more data. The limit on $B^0 \rightarrow K^{*0}\nu\bar{\nu}$ reported here is still one order of magnitude above the prediction of Buchalla et al. [1] and hence still allows room for substantial non-SM contributions.

We thank the KEKB group for the excellent operation of the accelerator, the KEK cryogenics group for the efficient operation of the solenoid, and the KEK computer group and the National Institute of Informatics for valuable computing and Super-SINET network support. We acknowledge support from the Ministry of Education, Culture, Sports, Science, and Technology of Japan and the Japan Society for the Promotion of Science; the Australian

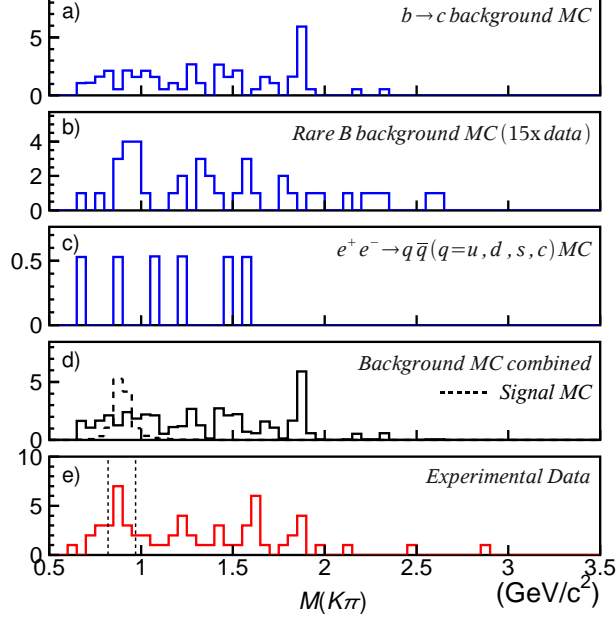


FIG. 4: The $M(K\pi)$ distributions from the events in the signal region, where a), b), c), d), and e) show the events from generic $b \rightarrow c$ MC, rare B MC, continuum $e^+e^- \rightarrow q\bar{q}$ ($q = u, d, c, s$) MC, background MC combined, and data, respectively. The dashed histogram in d) illustrates the distribution for $B^0 \rightarrow K^*\nu\bar{\nu}$ signal MC.

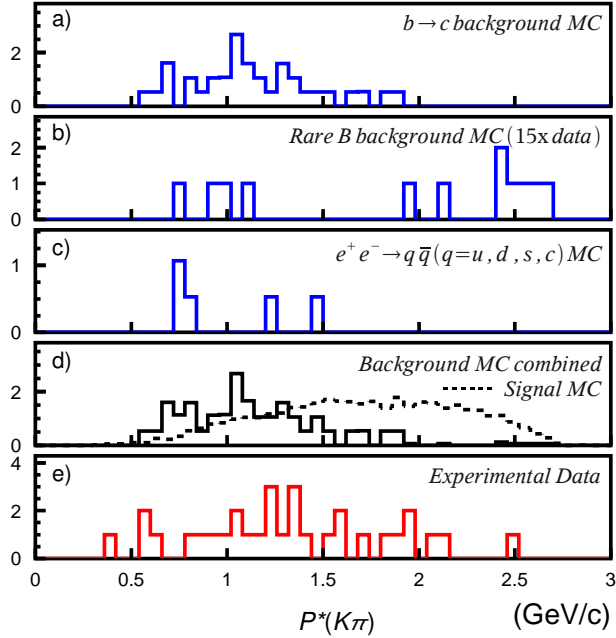


FIG. 5: The $P^*(K\pi)$ distributions (without Fisher requirement) from the events in the signal region, where a), b), c), d), and e) show the events from generic $b \rightarrow c$ MC, rare B MC, continuum $e^+e^- \rightarrow q\bar{q}$ ($q = u, d, c, s$) MC, background MC combined, and data, respectively. The dashed histogram in d) illustrates the distribution for $B^0 \rightarrow K^*\nu\bar{\nu}$ signal MC.

Research Council and the Australian Department of Education, Science and Training; the National Science Foundation of China and the Knowledge Innovation Program of the Chinese Academy of Sciences under contract No. 10575109 and IHEP-U-503; the Department of Science and Technology of India; the BK21 program of the Ministry of Education of Korea, and the CHEP SRC program and Basic Research program (grant No. R01-2005-000-10089-0) of the Korea Science and Engineering Foundation; the Polish State Committee for Scientific Research under contract No. 2P03B 01324; the Ministry of Science and Technology of the Russian Federation; the Slovenian Research Agency; the Swiss National Science Foundation; the National Science Council and the Ministry of Education of Taiwan; and the U.S. Department of Energy.



- [1] G. Buchalla, B. Hiller and G. Isidori, *Phys. Rev. D* **63**, 014015 (2001).
- [2] C. Bird, *Phys. Rev. Lett.* **93**, 201803 (2004).
- [3] K. Abe *et al.* (Belle Collaboration), hep-ex/0410006; M. Iwasaki *et al.* (Belle Collaboration), *Phys. Rev. D* **72**, 092005 (2005); B. Aubert *et al.* (BaBar Collaboration), *Phys. Rev. D* **73**, 092001 (2006); B. Aubert *et al.* (BaBar Collaboration), *Phys. Rev. Lett.* **93**, 081802 (2004).
- [4] A. Ishikawa *et al.* (Belle Collaboration), *Phys. Rev. Lett.* **96**, 251801 (2006).
- [5] W. Adam *et al.* (DELPHI Collaboration), *Z. Phys. C* **72**, 207 (1996).
- [6] S. Kurokawa and E. Kikutani, *Nucl. Instrum. Methods Phys. Res., Sect. A* **499**, 1 (2003).
- [7] A. Abashian *et al.* (Belle Collaboration), *Nucl. Instrum. Methods Phys. Res., Sect. A* **479**, 117 (2002).
- [8] J. Conrad, O. Botner, A. Hallgren and C. Perez de los Heros, *Phys. Rev. D* **67**, 012002 (2003)